DMD Fast Forward. Published on February 26, 2007 as doi:10.1124/dmd.106.014282
This article has not been copyedited and formatted. The final version may differ from this version.

DMD#14282

Cyp1b1 protein in the mouse eye during development: An immunohistochemical study

by

Dharamainder Choudhary, Ingela Jansson, Karim Rezaul, David K.M. Han, Mansoor Sarfarazi and John B. Schenkman

Departments of Pharmacology (D.C., I.J., J.B.S), Surgery (D.C., M.S.), and Cell Biology (K.R., D.K.M.H.), University of Connecticut Health Center, Farmington, CT 06030

Running title: Cyp1b1 in mouse eye ontogeny

Corresponding Author: John B. Schenkman

Department of Pharmacology, University of Connecticut Health Center

Farmington, CT 06070

Tel: (860) 679-3694

Fax: (860) 679-2473

Email: jschenkm@neuron.uchc.edu

Pages

Text, 9

Figures, 5

Tables, 0

References, 43

Word Count

Abstract 269 words

Introduction 756 words

Discussion 1618 words

Abstract

We show, for the first time, the spatio-temporal appearance of Cyp1b1 protein during mouse eye ontogeny. The protein was unambiguously identified in the adult mouse eye and newborn (P0) whole mouse microsomes, and shown to be localized in inner ciliary epithelium, corneal epithelium, retinal inner nuclear cells and ganglion cells. The enzyme protein was present in the lens epithelium adjacent to the developing ciliary body at 15.5 days post conception (E15.5) and was most strongly expressed during E17.5 - P07. Subsequently, it declined to very low levels. The protein was also expressed in the corneal endothelial cells adjacent to the ciliary body at 7 days postnatally (P07). Cyp1b1 was barely detectable in the inner ciliary epithelium before E17.5 but increased rapidly postnatally, reaching adult levels by P28. Levels of the enzyme protein in the corneal epithelium were seen from E15.5 onward, rising sharply, and after a decline at P07, was highest in the adult animal eye. The presence of Cyp1b1 protein in the inner nuclear layer of the retina was very low in the prenatal eye, rising rapidly postnatally, and was highest in the adult animal eye. In the ganglion cell layer of the retina it increased slowly from E15.5 to P07, and then rapidly reached adult levels. Interestingly, Cyp1b1 was not detected in the trabecular meshwork at any stage of development or in the adult eye. We conclude that the enzyme may play important roles in the normal eye development and function in mouse as in human, and that the mouse may prove to be an excellent model for determination of the roles of CYP1B1 in human eye development and function.

Cytochrome P450 forms are known to function as monooxygenases, with Families 1-3 serving as xenobiotic-metabolizing enzymes. Their presence in the embryo and in developing tissue has generally been considered in terms of metabolism of xenobiotics that might enter the organism, or as a cause of toxic, carcinogenic or teratologic response to uptake of certain environmental pollutants. However, the expression of these forms of cytochrome P450 in the embryo and fetus appears to have both temporal and spatial components (Choudhary et al., 2003), suggesting, that these effects are inherent to developmental roles for the enzymes (Nebert, 1991; Stoilov et al., 2001; Choudhary et al., 2003; Schenkman et al., 2003; Choudhary et al., 2004a).

CYP1B1, a form of Family 1 cytochrome P450, is a protein found in many classes of vertebrates, from bony fish to humans (http://drnelson.utmem.edu/nelsonhomepage.html). This presence of evolutionary-conserved orthologous forms of the protein would suggest some critical developmental process associated with the enzyme. Such evolutionary retention of structure might suggest conservation of function, and the use of comparisons between orthologous forms as a way to elucidate the manner in which the enzyme effects normal eye development. In earlier studies, truncating mutations in CYP1B1 were linked to a disease phenotype, primary congenital glaucoma (PCG), by this group (Stoilov et al., 1997). Subsequently, a number of other mutations in this protein were also linked to PCG (Bejjani et al., 1998; Stoilov et al., 1998; Plasilova et al., 1999). Recently, mutations in CYP1B1 have also been linked to two other types of structural defects in the eye, primary open angle glaucoma (POAG) and Peter's Anomaly (Edward et al., 2004). These data strongly implicate CYP1B1 in the ontogeny of the eye.

Cyp1b1 null mice ($Cyp1b1^{-/-}$) have been shown to have developmental abnormalities of the drainage structures of the eye similar to that found in PCG humans (Libby et al., 2003). Mouse and human CYP1B1 forms have an 81% overall sequence identity, and greater than 90%

sequence identity in the substrate recognition sites (Choudhary et al., 2004a). In two of these sites, SRS-2 and SRS-4 the sequence identity is 100% between the orthologs (Choudhary et al., 2004b). Experiments have been carried out to compare the metabolism of endogenous substrates of cytochrome P450 by human and mouse CYP1B1 orthologs in an attempt to determine whether there is also a retention of substrate and metabolite specificity. Based upon a comparison of metabolism of testosterone, progesterone and ß-estradiol by human and mouse orthologs of CYP1B1, we were able to eliminate these as the possible conserved substrates (Choudhary et al., 2004a). We were also able to exclude the lipid, arachidonate, which similarly was metabolized strongly by CYP1B1, but not by Cyp1b1 (Choudhary et al., 2004b).

The eye is the tissue with the highest concentration of vitamin A in the body (Luo et al., 2006), and deficiency results in eye developmental defects and visual impairment. At least a dozen forms of human cytochrome P450 have been shown to be capable of all-*trans*-retinoid metabolism at fairly good rates (Chen et al., 2000; McSorley and Daly, 2000; Zhang et al., 2000; Choudhary et al., 2004b). Both human and mouse orthologs were found to be capable of oxidizing all-*trans*-retinol to all-*trans*-retinal and then to all-*trans*-retinoic acid (Choudhary et al., 2004b), a potent morphogen involved in early development of the conceptus (Maden et al., 1998; Abu-Abed et al., 2002) and eye development (McCaffery et al., 1999; Mori et al., 2001). A comparison of metabolism of these compounds by the human and mouse CYP1B1 orthologs indicated Cyp1b1 to have a higher specific activity toward all-*trans*-retinol (ROL) than CYP1B1, while with all-*trans*-retinal (RAL) as substrate the human enzyme had a higher specific activity for conversion to all-*trans*-retinoic acid (RA) (Choudhary et al., 2004b); neither ortholog could metabolize RA. Thus, if the role of Cyp1b1 in eye involves retinoid metabolism, its function would be in synthesis rather than in elimination of an active agent. During the visual cycle, light

causes conversion and release of 11-*cis*-retinal as all-*trans*-retinal (McCaffery et al., 1996), part of which would be converted to all-*trans*-retinoic acid and subsequently inactivated in the retina. The lost RAL would have to be replaced, and perhaps CYP1B1 orthologs contribute toward this task. In the present study we examined the temporal and spatial location of the Cyp1b1 in mouse eye in an attempt to discern its role(s) in eye development and function. The retina proved to be one of three functionally distinct regions of the eye with high levels of Cyp1b1 expression. The other two regions include the cornea and the inner ciliary epithelium.

MATERIALS and METHODS

Mice

The National Institutes of Health guidelines and Association for Research in Vision and Ophthalmology statement for the Use and Care of Animals, and procedures approved by the Animal Care Committee of the University of Connecticut Health Center were followed in this study. Wild type mouse strains, C57BL/6J and Swiss-Webster (CFW), were obtained from The Jackson Laboratories (Bar Harbor, ME) and Charles River (Wilmington, MA), respectively. For developmental studies, the C57BL/6 mice were bred in our Center for Laboratory Animal Care under veterinary supervision.

Antibody preparation, western blotting

Mouse Cyp1b1 was heterologously expressed in *Escherichia* coli DH5α transformed with pCWori^{+} plasmids containing the open reading frame of the mouse transcript modified for optimal expression in the same manner as the human CYP1B1 ortholog (Jansson et al., 2000). The purified protein prepared from the bacterial membrane fragments (Choudhary et al., 2004a) was used to generate antibodies in male New Zealand rabbits. Pre-immunization serum was collected from each animal for use as negative controls. The sera were diluted appropriately with

0.15 M NaCl containing 6.4 mM sodium phosphate, pH 7.2 (PBS), for use in western blotting and immunohistochemistry. Microsomes and tissue sample proteins were separated by sodium dodecylsulfate (SDS) polyacrylamide gel electrophoresis (PAGE) for western blotting as described earlier (Jansson et al., 2000), using Bio-Rad Mini-Protean II cell with 5 mm track widths. The Bio-Rad Mini-Trans Blot cell was used for protein transfer to the nitrocellulose membrane. The specificity and sensitivity of the antibody is described in the Results section.

Immunoinhibition of 7,12-dimethylbenz(α)anthracene (DMBA) metabolism

Rabbit anti-Cyp1b1 serum or pre-immune serum (30-150 µl) was preincubated with a reconstituted system containing 0.15 nmol of purified Cyp1b1 for 30 min at room temperature before starting the DMBA metabolism assay. The pre-immune serum was without affect on the activity. The reconstituted system consisted of purified cytochrome P450 reductase, Cyp1b1 and DLPC liposomes at 1:1:160 molar ratio, prepared as described (Jansson et al., 1985). DMBA metabolism was assayed as described in detail (Choudhary et al., 2004b), measuring metabolite peaks eluting from the HPLC column at 285 nm.

Protein identification by mass spectrometry

Cyp1b1 protein bands were excised from SDS-PAGE gels and subjected to in-gel tryptic digestion as previously described (Rezaul et al., 2005). Digestions were carried out for 18 h at 37 ^{o}C with sequencing grade trypsin (Promega, Madison, WI). Peptides from each gel band were extracted, and the peptide digests were then sequenced using a high throughput tandem mass spectrometer (LTQ- ion trap, ThermoFinnigan, San Jose, CA) equipped with a nanoelectrospray reversed phase liquid chromatography interface. Data were acquired in automated MS/MS mode using the data acquisition software provided with the mass spectrometer to detect and sequence each peptide as it eluted from the column. The dynamic exclusion and isotope exclusion

functions were employed to increase the number of peptide ions that were analyzed. MS/MS data was then analyzed and matched to protein sequences in the National Center for Biotechnology Information (NCBI) database using the SEQUEST search engine. For Protein identification, SEQUEST score was set for 1.8, 2.2 and 3.7 for +1, +2, and +3 charge-state peptide respectively.

Histology and immunohistochemistry

Eyes of 6 month old (P6mo) C57BL/6J and albino Swiss Webster (CFW) mice, and 1 month old (P28) C57BL/6J mice were removed, fixed, and embedded in paraffin. Heads of 15 day post-conception (E15.5) and E17.5 mouse fetuses and whole E12.5 embryos were similarly treated. Deparaffinized slices of 5 μm thickness were fixed to slides and stained with hematoxylin/eosin (H&E) or the non-biotin-avidin DAKO+ two-step immunohistochemical system. The latter slides were then incubated with DAKO Peroxidase Block (Envision, St. Louis, MO) to quench endogenous peroxidase activity and then reacted with 50 μl of rabbit pre-immune or antiserum raised to mouse Cyp1b1, at 1:500 or 1:1000 dilution in PBS, at room temperature for 2 hr. This was followed by incubation with a horse radish peroxidase-complexed polymer (Dako Envision+ system) for 30 min. Color was developed with VIP peroxidase substrate (Vector Labs, Youngstown, OH) for 6 min at room temp, followed by washing and counterstaining with methylgreen. Slides were photographed at 400x magnification. Histology was performed over a 1½ year period and images were obtained using different equipment, resulting in differences in background color development. In order to visualize changing levels of Cyp1b1 with development, immunostaining was assessed by 3 persons in the laboratory, who viewed 3 - 4 slides of each developmental time point chosen and rated the intensity of VIP staining in the different eye structures on a scale of 0-10.

In considering the spatio-temporal expression of Cyp1b1 in the development of the mouse eye, advantage was taken of the very excellent developmental images provided in the online embryology tutorial of Drs. Sulik and Bream at the University of North Carolina, Chapel Hill (http://www.med.unc.edu/embryo_images/), the Atlas of Mouse Development (Kaufman, 2003).

RESULTS

Identification of Cyp1b1 in the mouse eye

Examination of the transcript expression level profiles of the 62 mouse Cyp forms of P450 families 1-3 using the UniGene EST Profile Viewer (http://www.ncbi.nlm.nih.gov/UniGene/UGOrg.cgi?TAXID=10090) revealed the presence of 12 of these forms in the eye. These include Cyp1b1, Cyp2b10, CYP2b13, Cyp2c29, Cyp2d22, Cyp2w1, Cyp3a13, Cyp3a25, as well as Cyp2f2, Cyp2g1, Cyp2j6 and Cyp2j13. The expression levels (transcript frequencies) of these Cyps/10^6 transcripts lie between 5 and 15, except for Cyp1b1, which has an expression frequency of 75/10^6 transcripts. The relative transcript levels of CYP1B1 and Cyp1b1 in the human and mouse eye are 5-fold higher than other cytochrome P450 forms and of those shown to metabolize the all-trans-retinoids, only CYP1B1 has an orthologous form found in the mouse. In examining the sequence identities of these mouse proteins in alignment with Cyp1b1, it would appear that the latter four (Cyp2f2, Cyp2g1, Cyp2j6 and Cyp2j13) lack any contiguous clusters of 5 or more residues in common with Cyp1b1. Of the rest of the forms, Cyp2b10 and Cyp2d22 each have two sequence clusters of 5 residues that align with Cyp1b1, while the others have only one. Since linear epitopes are considered to contain at least 8-10 amino acids one might expect low probability of cross reactivity with anti-Cyp1b1 antibodies. Overall sequence identities between Cyp1b1 and these 11 forms range from

27% to 35%, which, when taken with the sequence cluster information would also indicate a low probability of reaction with antibodies raised against Cyp1b1.

The EST profile of Cyp2b10 would suggest a location only in the eye for this form. In contrast, Cyp2d22 has a transcript frequency in liver more than 25 fold greater than its frequency in the eye. Cyp1b1 transcript frequency in liver was about 10% of its frequency in the eye, and Cyp1b1 protein was not detected in liver microsomes using antibodies to Cyp1b1 (**Figure 1A, left**, track 3**)**. Antibodies to Cyp1b1 did not cross-react with nor reveal any of the other cytochrome P450 forms in the liver microsomes (**Figure 1A, left**, track 3). The antibody did, however, detect a considerable amount of Cyp1b1 protein in mouse breast tumor 600 x g supernatant (**Figure 1A, left**, track 2), and much smaller amounts in microsomes of the P0 mouse (**Figure 1, left**, track 4). Cyp1b1 protein was-barely detected in adult eye microsomes (**Figure 1A, left**, track 1). The level of Cyp1b1 protein in these latter two microsomal preparations was extremely low, and difficult to demonstrate by western blotting without enhancing the background staining. Based upon the stain density of the purified Cyp1b1 in western blot titrations, from 200 fmol-5 fmol (**Figure 1A**, **right**), the amount of Cyp1b1 in the P0 mouse microsomes (track 4, left) was estimated to be less than 5 fmols, or below 0.2 pmol/ mg microsomal protein, and even lower in the adult eye microsomes. To demonstrate the protein in tissue fractions or homogenates by western blotting involves spreading of the enzyme throughout the homogenate, and thus its dilution from localized sites. This required extended development time for visualization of the very low content of reactive protein, which also increased non-specific background staining, and necessitated confirmation of reactive band identity.

DMD Fast Forward. Published on February 26, 2007 as DOI: 10.1124/dmd.106.014282
This article has not been copyedited and formatted. The final version may differ from this version.

We set out to confirm the identity of the antibody-reactive protein band in microsomes as Cyp1b1. The band in a track containing purified Cyp1b1, was excised from the polyacrylamide gel, the protein cleaved with trypsin as indicated in Methods, and subjected to LC/MS/MS analysis. The samples of purified Cyp1b1 excised from the gel generated 18 ion fragments (**Figure 1B,** top**)**, each recognized in NCBI Blast sequence search as belonging to Cyp1b1. The sequences recognized as Cyp1b1 are shown in **Figure 1B** (bottom) and are in bold type.

Adult mouse eye microsomal samples (50 μg) were applied to each of three separate tracks of an SDS-PAGE alongside a track containing purified Cyp1b1. The region of the gel corresponding to the antibody-responsive band was excised from two of the tracks for LC/MS/MS determination of Cyp1b1 presence. The most abundant unique ion fragment found, ALASSVMIFSVGKR, was successfully identified in the gel digest from the adult eye microsomes, corresponding to Cyp1b1 residues 455-468 (**Figure 1B**, bottom), confirming the identity of the protein in the eye revealed by the antibody.

P0 whole mouse microsomes were similarly subjected to SDS-PAGE and the region of tracks corresponding to the antibody-reactive band were excised, treated with trypsin; and examined by LS/MS/MS. The proteolytically treated band yielded an ion fragment, MH+, of 1462.1072 m/z (**Figure 1B**, middle) that had the amino acid sequence of SLAFGHYSEHWK. This sequence corresponded to residues 131-142 of the Cyp1b1 sequence (**Figure 1B**, bottom, underlined bold) in the NCBI Blast search, confirming the identity and presence of Cyp1b1 protein in the P0 mouse microsomes.

The antibody was inhibitory of DMBA metabolism, with increasing amounts of inhibition resulting from increasing concentrations of antibody; activity dropped to 70% at 150 μl antiserum/ml of assay medium containing 0.15 nmol of Cyp1b1.

DMD Fast Forward. Published on February 26, 2007 as DOI: 10.1124/dmd.106.014282
This article has not been copyedited and formatted. The final version may differ from this version.

Immunohistochemical determination of Cyp1b1 distribution in eye with age in the postnatal mouse

Adult (6 month old, P6mo) C57BL/6 mouse eyes were examined for the presence of Cyp1b1 protein by immunohistochemistry. The Cyp1b1 protein was detected by appearance of reddish-purple color, and the color was not observed with pre-immune serum. Attempts to show removal of reacting antibodies by prior incubation of the antiserum with purified Cyp1b1 protein were thwarted by binding of the antibody treated protein to the tissue, thereby giving an increased signal. **Figure 2** shows the localization of Cyp1b1 protein in the iridiocorneal (IC) angle region associated structures. In agreement with our earlier report indicating the presence of Cyp1b1 in adult mouse eye (Choudhary et al., 2006) and studies on distribution of CYP1B1 in human eye (Doshi et al., 2006), the protein stain could not be demonstrated in the trabecular meshwork (TM). The pigment was quite dense in the corneal epithelium (C), inner ciliary epithelium (ICE), retinal ganglion cells (G) and inner nuclear layer of the retina (IN). Staining intensity and patterns in the different regions varied in the retinal ganglion cells positive responses appeared punctate and strong (**Figure 2**). Similar localization of stain was seen in the inner ciliary epithelium (ICE), but stain also was spread through the cells, giving the cytoplasm a pink cast. In contrast, although reacting strongly, the distribution of stain in the corneal epithelial cells was more diffuse and spread throughout the cytoplasm. **Figure 3** shows the immunohistochemical staining of regions of the eyes of mice from 6 month old adult (P6mo) to 14-day (P14) postnatal age. As shown in **Figure 3**, a-c, in eyes of the 6 month old C57BL/6 mouse, a considerable amount of Cyp1b1 was present, seen as diffuse staining in the anterior corneal epithelium (**Figure 3,** a); staining was absent in the corneal stroma between Bowman's membrane and Descemet's membrane and the keratinocyte cells contained therein. The inner

ciliary epithelium proximal to the retina and before the iris showed both punctate and diffuse purple stain (**Figure 3,** b), indicating the presence of Cyp1b1. The pigment of the outer ciliary epithelium prevented determination of the presence of Cyp1b1 staining in these cells. Attempts to bleach the pigment with hydrogen peroxide did not yield usable data. The ganglion cell layer and the inner nuclear layer of the retina exhibited dense, punctate staining for Cyp1b1 (**Figure 3,** c).

In order to determine whether outer ciliary epithelium expressed Cyp1b1, we examined the eyes of the 6 month old albino Swiss Webster mouse. **Figure 3** (d-f) indicates the expression pattern of Cyp1b1 in these eyes was similar to that in the C57BL/6 mouse eye. The variable distribution of the enzyme in different ocular structures of the eye tissue is very apparent in these sections. The anterior corneal epithelial cells (**Figure 3,** d), the inner ciliary epithelial cells (**Figure 3,** e, ICE), the ganglion cells (**Figure 3,** f, G) and the inner nuclear cells (**Figure 3,** f, IN) all show the presence of Cyp1b1. No clear indication was found for its presence in the outer ciliary epithelium (**Figure 3,** e, OCE). As with the C57BL/6 mouse eyes, no staining was seen in the TM cells.

Immunohistochemical determination of Cyp1b1 in regions of the immature mouse eye

Although much of eye development occurs prenatally, major developmental changes in the anterior chamber region of the eye occur postnatally (Pei and Rhodin, 1970). By 28 days of postnatal age (P28) the eye structures appeared like that of the adult eye**,** and Cyp1b1 protein was similarly distributed (**Figure 3,** g-i), although the intensity of staining was not as high. Staining was strongest in the retina (**Figure 3,** i). In the P14 mouse eye (**Figure 3**, j-l), the distribution of Cyp1b1 was also similar to that in the P6mo mouse eye and of lower concentration.

In the P07 mouse eye (**Figure 4,** a-c) the epithelial cells of the cornea (C), the inner ciliary epithelial cell layer (ICE), the ganglion cells (G) and inner nuclear cells (IN), stained much less for Cyp1b1 than in older eyes, but interestingly, a relatively high level of enzyme was found in the corneal endothelial cells (**Figure 4** a, EN, arrow) and the lens anterior epithelial cells (**Figure 4** b, L, arrow), both in regions adjacent to the ciliary body. The distinctive trabecular meshwork structure of alternating bands of cells and stroma is not yet apparent at this age.

In the P01 mouse eye (**Figure 4,** d-f) the ciliary process appeared as a bulge of pigmented retinal cells with a slight projection anterior to the lens. The bulge is coated with columnar cells extending from the non-pigmented, neural retinal layer (ICE). Cyp1b1 staining was faintly detected in the eye structures, such as cornea (**Figure 4** d, arrow), ICE (**Figure 4** e, arrow) and retinal ganglion cells (**Figure 4** f, arrows). Cyp1b1 was also present in elevated levels in the lens epithelial cells (**Figure 4** e, arrow), in the region of the developing ciliary process.

Immunohistochemical determination of Cyp1b1 in regions of the developing mouse eye in utero

At 17.5 days post conception (E17.5) the structure of the eye has partially formed, with the lens present and containing an anterior epithelial cell layer (**Figure 4**, g, EC) which is absent posterior toward the end of the optic cup. The tip of the optic cup contains a fusion of the pigmented retinal cells (PR) with the neuroblastic retinal cells (NR) of the retina (**Figure 4** h) and is slightly enlarged, forming an angle with the cornea. The ciliary body and iris have not yet formed. The anterior epithelial cell layer of the cornea contains a diffuse low amount of Cyp1b1 (arrow), especially near the developing ciliary body, and faint staining is also seen in the

adjacent lens epithelial cells (**Figure 4**, h, arrows). Low levels of Cyp1b1 are detectable in the ganglion cell layer of the retina (**Figure 4** i**,** arrow).

Distribution and levels of Cyp1b1 in the E15.5 eye were similar to that in the E17.5 eye. At E15.5 the structures of the eye are even less well defined. There is a fusion of the neuroblastic retinal cells (NR) and pigmented retinal cells at the anterior end of the optic cup (**Figure 4,** k). The anterior corneal epithelial cells are readily seen over a multi-layered structure and contain low levels of Cyp1b1 (**Figure 4**, j, k, arrows). In some sections, the eyelids (EL), containing Cyp1b1, are seen, and are fused above the cornea, creating a conjunctival space (**Figure 4,** j). Cyp1b1 could be detected at E15.5 in the retinal ganglion cells (**Figure 4,** l) and corneal epithelium (**Figure 4** k, arrows). Anterior lens epithelial cells in the region of the developing iris and prospective ciliary body also stain faintly for Cyp1b1 (not shown).

Figure 5 shows the trend in changes in the levels of Cyp1b1 in the different structures of the eyes of mouse at different ages, based upon relative intensity of staining. Levels of Cyp1b1 in the ganglion cell layer appeared to be highest in animals from P14 development to adult (6 months), and are sharply lower at earlier ages, especially during *in utero* development. Levels of the Cyp1b1 protein in the inner nuclear layer of the retina approached the limits of detection at period earlier than P07, being sharply elevated from P14 onward. While levels of Cyp1b1 in the corneal epithelial cells were highest during postnatal development after P07, its level in the adult was greatly elevated from that of P28 cornea. Levels of Cyp1b1 in the inner ciliary epithelium appeared to parallel development of the ciliary body following appearances of the ciliary processes from P14. As the lens develops, Cyp1b1 is found in the anterior epithelial cells, especially adjacent to the developing ciliary body. Levels rise at E17.5 and are high adjacent to the developing ciliary process through P01 and P07, declining thereafter following formation of

the ciliary processes. Concomitant with the rise in levels in the lens is the appearance of Cyp1b1 in the endothelial cells at P07 (**Figure 4**, a). Its presence in this location was not detected at other ages.

At E12.5 several major structures of the eye are in the process of development. The lens is still forming, and is separate from the retina by the hyaloid cavity. The outer corneal ectodermal layer overlays a thicker band of loose mesenchymal cells and the lens vesicle is present. Attempts to identify Cyp1b1 at this stage of development by immunohistochemistry were questionable. Faint staining was seen for Cyp1b1 in some sections, but stain was not always clearly identifiable with cells.

DISCUSSION

Mutations causing homozygous inactivation of CYP1B1 have been linked to the disease phenotype of primary congenital glaucoma (PCG) (Stoilov et al., 1997; Bejjani et al., 1998; Stoilov et al., 1998; Belmouden et al., 2002). In the $Cyp1b1^{-/-}$ mouse no gross abnormalities or elevated intraocular pressure were observed. However, angle abnormalities involving TM were seen in the $Cyp1b1^{-/-}$ mouse eye, including corneal basement membrane impinging on or overlaying the TM or deficiencies in the Schlemm canal in some sections (Libby et al., 2003).

Development of the murine eye occurs relatively late in gestation, with most of the anterior chamber structures development occurring postnatally. The optic vesicle appears on day 8 of gestation (E8) (Kaufman, 2003) with a cluster of cells in the rostral part of the anterior neural plate of the forebrain. Earlier, we failed to see evidence of Cyp1b1 mRNA transcripts at E7 (Choudhary et al., 2003). However, Cyp1b1 transcripts could be seen in eye by E9.5 using *in situ* hybridization (Stoilov et al., 2004), well before the development of the anterior chamber structures. The neural ectoderm of the optic vesicle approaches and induces the surface ectoderm

to form the lens placode, which becomes the lens vesicle, and the optic vesicle part of the neural ectoderm forms the lens cup, which differentiates into two retinal layers by E12, the neural retina and the future pigmented retinal epithelium. Although RT-PCR experiments clearly showed the presence of mRNA transcripts at this stage of ontogeny (Choudhary et al., 2003), Cyp1b1 protein in the eye tissue was at a level just barely, and not consistently, detectable at E12.5 by immunohistochemical analyses. The approach of the lens to the surface ectoderm appears to induce corneal and anterior chamber formation, and the development of the ciliary body (Beebe, 1986). By E15 there is a distinctive tapering of the anterior optic cup to an inner neural and outer pigmented region, forming a boundary from which the iris and ciliary body will appear (Napier and Kidson, 2005). Cyp1b1 transcripts have been seen in the developing mouse embryo at E15.5 (Choudhary et al., 2005), and in the E15 mouse retina (Bejjani et al., 2002), and at this stage of development Cyp1b1 protein is readily located in the eye structures (**Figures 4, 5**).

In the present study, polyclonal antibodies to mouse Cyp1b1 demonstrated the presence of that protein in mouse breast tumor tissue, newborn whole mouse microsomes, and in adult eye microsomes. The antibody was capable of inhibition of DMBA metabolism by purified Cyp1b1 by about 30%, an observation consistent with the observed non-inhibitory to variable levels of inhibition of other forms of cytochrome P450 by monoclonal antibodies (Gelboin et al., 1995; Gelboin et al., 1996). In agreement with an earlier report that levels of CYP1B1 could not be immunodetected in normal human tissues (McFadyen et al., 1999), the ortholog Cyp1b1 was not detected in mouse liver microsomes, and required prolonged development to detect the low fmol levels present in newborn mouse microsomes and adult mouse eye microsomes. The protein detected in these latter tissues was unambiguously identified by LC/MS/MS. The antibody was used for detection of this protein localized in the eye structures. In agreement with earlier reports

that human tumors have elevated levels of CYP1B1 protein (Murray et al., 1997), we could show elevated levels in mouse breast tumors. The eye has three functionally different regions, the corneal region, the anterior chamber region, and the retinal region. Using immunohistochemical procedures, Cyp1b1 protein could be shown in substructures of all of these regions.

The ciliary processes begin to form by E18.5 in the anterior edge of the optic cup. By P01, the first day after birth, to P02, a faster proliferation of the outer ciliary epithelium appears to initiate the formation of the ciliary process, resulting in a discrete body by P07 (Napier and Kidson, 2005). Interestingly, between E17.5 and P07, Cyp1b1 protein was at very low levels in the corneal epithelium, but was elevated in anterior lens epithelium (**Figure 5**). Further, the presence of Cyp1b1 protein could be shown in the corneal endothelial cells in the region adjacent to the developing ciliary body at P07 **(Figure 4)**. The lens has been shown to influence development of adjacent ocular structures like the ciliary body (Beebe, 1986). The transient appearance of Cyp1b1 in the corneal endothelial cells and in the anterior lens epithelium suggests a role for the hemoprotein in development of the ciliary body. By P14 the protein has begun to increase in the inner ciliary epithelium and the rest of the eye structures, and to decline in the lens. The location of Cyp1b1 in the different eye structures at P28 mirrors the distribution in the adult mouse eye, although levels-were lower. Similarly, the iridiocorneal angle does not reach maturity until 2 months of age (Smith et al., 2001). Cyp1b1 protein was not found in the TM of the adult mouse eye (**Figure 2**), nor in the region of its development from P28 or earlier, in agreement with a similar observation in the human eye (Doshi et al., 2006). We suspect that Cyp1b1 in structures adjacent to the TM may act to modulate levels of some endobiotic metabolite in the anterior chamber fluid that influences development and later modulates the function of the TM.

The cornea, formed from the outer epidermal layer and the inner neural crest cells begins to resemble the mature cornea by E15 (Pei and Rhodin, 1970). Cyp1b1 protein was found in the outermost epithelial cell layer of the forming cornea as well as in the sclera from which it extends; Cyp1b1 protein was not seen in the inner stromal layers of the cornea. Levels of Cyp1b1 in the corneal epithelium begin to rise at 2 weeks postnatally. Appreciable levels were seen at P14-P28, but the level was dramatically increased in the 6-month-old mouse eye (**Figure 3**). The lens interfaces with the environment. We suspect that Cyp1b1 may serve in a xenobiotic metabolizing role in this structure. It is possible that exposure to body wastes plus rising steroid levels as the animals mature may serve to dramatically elevate (induce) the Cyp1b1 levels in the cornea, serving as protection against environmental agents impacting the eye.

The body of the retina appears as an inner neuroblastic layer and a denser outer neuroblastic layer (Pei and Rhodin, 1970). By E17.5 there is a distinct dense nuclear layer and a less dense ganglion cell layer anterior to it. By P01 the nuclear layer develops into a denser outer nuclear layer and a less dense inner nuclear layer underlying the retinal ganglion cells. While at P01 the presence of Cyp1b1 was barely detectable in the inner nuclear layer of the retina, by P07 it was present in modest amount (**Figure 4**). Levels in the ganglion cell layer were higher than the inner nuclear layer and levels in both layers increased dramatically in content by P14 to adult levels. The hemoprotein was not detectable in the outer nuclear layer of the retina at any age investigated. We suspect that the presence of Cyp1b1 in the retina may have a different function than for the cornea and for the anterior chamber structures.

In the visual cycle the light absorbing chromophore, 11-*cis*-retinal, is converted by absorption of a photon to RAL which dissociates from the opsin and is rapidly converted to all-*trans*-retinoic acid (RA), an irreversible reaction (McCaffery et al., 1996). RA, a potent

morphogen, is rapidly inactivated by a family of CYP26 enzymes located in the eye (Luo et al., 2006). A portion of the RAL is recovered in the retinal pigmented epithelium by an isomerase enzyme that re-forms 11-*cis*-retinal (Mata et al., 2005). The retinal protein Rpe65 has been purified from bovine retina and shown to have isomerase activity, aiding in converting RAL to 11-*cis* retinal (Jin et al., 2005) Its direct role in cone pigment regeneration remains controversial, but death of photoreceptor cells occurs in the $Rpe65^{-/-}$ mouse (Cottet et al., 2006). The presence of Cyp1b1 in the retina may indicate a role in the maintenance or replenishment of RAL lost during the visual cycle. Alternatively, or perhaps in addition, the hemoprotein may serve to protect against potentially toxic lipophilic compounds that reach the retina. Further studies on this potential role of CYP1B1 orthologs and its precise cellular localization in the retina should help elucidate its role in retinal functions.

The present study is in agreement with recent reports in which the immunolocalization of CYP1B1 has been reported in human adult and fetal eyes (Doshi et al., 2006) and in adult mouse eye (Choudhary et al., 2006). In those studies CYP1B1 protein was reported to be present in the inner ciliary epithelium and corneal epithelium, but to be absent from the outer ciliary epithelium and TM. Some differences between the former study and the present study include the reported presence of CYP1B1 protein in the human corneal keratinocytes and the pigmented epithelium of iris and retina. Cyp1b1 protein was not detected in these regions of the mouse eye at any stage of development in the present studies. However, *in situ* hybridization experiments have shown the presence of Cyp1b1 transcripts in the pigmented ciliary epithelium as well as in the neural retina of the E15.5 mouse eye (Bejjani et al., 2002).

The present report supports our suggestions (Jansson et al., 2001; Stoilov et al., 2001; Choudhary et al., 2003; Schenkman et al., 2003; Choudhary et al., 2004a; Choudhary et al.,

2004b; Stoilov et al., 2004; Choudhary et al., 2005; Choudhary et al., 2006) that the existence of the orthologous forms of cytochrome P450 and their presence in ontogeny may be an indication of roles other than in xenobiotics metabolism for these enzymes, such as in development, and perhaps physiological function.

Acknowledgements

The authors thank Dr. John Peluso, Department of Cell Biology, University of Connecticut Health Center, for helpful discussions and for allowing us the use of his microscopic equipment, and Ms. Nancy Ryan for her help in enhancing the effectiveness of the immunohistochemistry.

References

Abu-Abed S, MacLean G, Fraulob V, Chambon P, Petkovich M and Dolle P (2002) Differential expression of the retinoic acid-metabolizing enzymes CYP26A1 and CYP26B1 during murine organogenesis. *Mech. Dev.* **110:**173-177.

Beebe DC (1986) Development of the ciliary body: a brief review. *Trans. Ophthalmol. Soc. U.K.* **105:**123-130.

Bejjani BA, Lewis RA, Tomey KF, Anderson KL, Dueker DK, Jabak M, Astle WF, Otterud B, Leppert M and Lupski JR (1998) Mutations in CYP1B1, the gene for cytochrome P450 1B1, are the predominant cause of primary congenital glaucoma in Saudi Arabia. *Am. J. Hum. Genet.* **62:**325-333.

Bejjani BA, Xu L, Armstrong D, Lupski JR and Reneker LW (2002) Expression patterns of cytochrome P4501B1 (Cyp1b1) in FVN/N mouse eyes. *Exp. Eye Res.* **75:**249-257.

Belmouden A, Melki R, Hamdani M, Zaghloul K, Amraoui A, Nadifi S, Akhayat O and Garchon HJ (2002) A novel frameshift founder mutation in the cytochrome P450 1B1 (CYP1B1) gene is associated with primary congenital glaucoma in Morocco. *Clin. Genet.* **62:**334-339.

Chen H, Howald WN and Juchau MR (2000) Biosynthesis of all-trans-retinoic acid from all-trans-retinol: Catalysis of all-trans-retinol oxidation by human P-450 cytochromes. *Drug Metab. Dispos.* **28:**315-322.

Choudhary D, Jansson I, Sarfarazi M and Schenkman JB (2004a) Xenobiotic-metabolizing cytochromes P450 in ontogeny: evolving perspective. *Drug Metab. Rev.* **36:**547-566.

Choudhary D, Jansson I, Sarfarazi M and Schenkman JB (2006) Physiological significance and expression of P450s in the developing eye. *Drug Metab. Rev.* **38:**337-352.

Choudhary D, Jansson I, Schenkman JB, Sarfarazi M and Stoilov I (2003) Comparative expression profiling of 40 mouse cytochrome P450 genes in embryonic and adult tissues. *Arch. Biochem. Biophys.* **414:**91-100.

Choudhary D, Jansson I, Stoilov I, Sarfarazi M and Schenkman JB (2004b) Metabolism of retinoids and arachidonic acid by human and mouse cytochrome P450 1B1. *Drug Metab. Dispos.* **32:**840-847.

Choudhary D, Jansson I, Stoilov I, Sarfarazi M and Schenkman JB (2005) Expression patterns of mouse and human CYP orthologs (families 1-4) during development and in different adult tissues. *Arch. Biochem. Biophys.* **436:**50-61.

Cottet S, Michaut L, Boisset G, Schlecht U, Gehring W and Schorderet DF (2006) Biological characterization of gene response in Rpe65-/- mouse model of Leber's congenital amaurosis during progression of the disease. *Faseb J* **20:**2036-2049.

Doshi M, Marcus C, Bejjani BA and Edward DP (2006) Immunolocalization of CYP1B1 in normal, human, fetal and adult eyes. *Exp. Eye Res.* **82:**24-32.

Edward D, Al Rajhi A, Lewis RA, Curry S, Wang Z and Bejjani B (2004) Molecular basis of Peters anomaly in Saudi Arabia. *Ophthalmic Genet.* **25:**257-270.

Gelboin HV, Goldfarb I, Krausz KW, Grogan J, Korzekwa KR, Gonzalez FJ and Shou M (1996) Inhibitory and noninhibitory monoclonal antibodies to human cytochrome P450 2E1. *Chem. Res. Toxicol.* **9:**1023-1030.

Gelboin HV, Krausz KW, Goldfarb I, Buters JTM, Yang SK, Gonzalez FJ, Korzekwa KR and Shou M (1995) Inhibitory and non-inhibitory monoclonal antibodies to human cytochrome P450 3A3/4. *Biochem. Pharmacol.* **50:**1841-1850.

Jansson I, Mole J and Schenkman JB (1985) Purification and characterization of a new form (RLM2) of liver microsomal cytochrome P-450 from untreated rat. *J. Biol. Chem.* **260:**7084-7093.

Jansson I, Stoilov I, Sarfarazi M and Schenkman JB (2000) Enhanced expression of CYP1B1 in Escherichia coli. *Toxicology* **144:** 211-219.

Jansson I, Stoilov I, Sarfarazi M and Schenkman JB (2001) Effect of two mutations of human CYP1B1, G61E and R469W, on stability and endogenous steroid substrate metabolism. *Pharmacogenetics* **11:**793-801.

Jin M, Li S, Moghrabi WN, Sun H and Travis GH (2005) Rpe65 is the retinoid isomerase in bovine retinal pigment epithelium. *Cell* **122:**449-459.

Kaufman MH (2003) *The atlas of mouse development.* Academic Press, San Diego.

Libby RT, Smith RS, Savinova OV, Zabaleta A, Martin JE, Gonzalez FJ and John SW (2003) Modification of ocular defects in mouse developmental glaucoma models by tyrosinase. *Science* **299:**1578-1581.

Luo T, Sakai Y, Wagner E and Drager UC (2006) Retinoids, eye development, and maturation of visual function. *J Neurobiol* **66:**677-686.

Maden M, Sonneveld E, van der Saag RT and Gale E (1998) The distribution of endogenous retinoic acid in the chick embryo: implications for developmental mechanisms. *Development* **125:**4133-4144.

Mata NL, Ruiz A, Radu RA, Bui TV and Travis GH (2005) Chicken retinas contain a retinoid isomerase activity that catalyzes the direct conversion of all-trans-retinol to 11-cis-retinol. *Biochemistry (Mosc).* **44:**11715-11721.

McCaffery P, Mey J and Drager UC (1996) Light-mediated retinoic acid production. *Proc Natl Acad Sci U S A* **93:**12570-12574.

McCaffery P, Wagner E, O'Neil J, Petkovich M and Drager UC (1999) Dorsal and ventral retinal territories defined by retinoic acid synthesis, break-down and nuclear receptor expression. *Mech. Dev.* **82:**119-130.

McFadyen MCE, Breeman S, Payne S, Stirk C, Miller ID, Melvin WT and Murray GI (1999) Immunohistochemical localization of cytochrome P450 1B1 in breast cancer with monoclonal antibodies specific for CYP1B1. *J. Histochem. Cytochem.* **47:**1457-1464.

McSorley LC and Daly AK (2000) Identification of human cytochrome P450 isoforms that contribute to all-*tran*-retinoic acid 4-hydroxylation. *Biochem. Pharmacol.* **60:**517-526.

Mori M, Ghysellinck NB, Chambon P and Mark M (2001) Systematic immunolocalization of retinoid receptors in developing and adult mouse eyes. *Invest. Ophthalmol. Vis. Sci.* **42:**1312-1318.

Murray GI, Taylor MC, McFadyen MC, McKay JA, Greenlee WF, Burke MD and Melvin WT (1997) Tumor-specific expression of cytochrome P450 CYP1B1. *Cancer Res.* **57:**3026-3031.

Napier HRL and Kidson SH (2005) Proliferation and cell shape changes during ciliary body morphogenesis in the mouse. *Dev. Dyn.* **233:**213-223.

Nebert DW (1991) Proposed role of drug-metabolizing enzymes: regulation of steady state levels of the ligands that effect growth, homeostasis, differentiation, and neuroendocrine functions. *Mol. Endocrinol.* **5:**1203-1214.

Pei YF and Rhodin JAG (1970) The prenatal development of the mouse eye. *Anat. Rec.* **168:**105-126.

Plasilova M, Stoilov I, Sarfarazi M, Kadasi L, Ferakova E and Ferak V (1999) Identification of a single ancestral CYP1B1 mutation in Slovak Gypsies (Roms) affected with primary congenital glaucoma. *J. Med. Genet.* **36:**290-294.

Rezaul K, Wu L, Mayya V, Hwang SI and Han D (2005) A systematic characterization of mitochondrial proteome from human T leukemia cells. *Mol Cell Proteomics* **4:**169-181.

Schenkman JB, Choudhary D, Jansson I, Sarfarazi M and Stoilov I (2003) Involvement of cytochromes P450 in development. *Proc. Indian Natnl. Sci. Acad. B* **69:**917-929.

Smith RS, Zabaleta A, Savinova OV and John SW (2001) The mouse anterior chamber angle and trabecular meshwork develop without cell death. *BMC Developmental Biology* **1:**3.

Stoilov I, Akarsu AN, Alozie I, Child A, Barsoum-Homsy M, Turacli ME, Or M, Lewis RA, Ozdemir N, Brice G, Aktan SG, Chevrette L, Coca-Prados M and Sarfarazi M (1998) Sequence analysis and homology modeling suggest that primary congenital glaucoma on 2p21 results from mutations disrupting either the hinge region or the conserved core structures of cytochrome P4501B1. *Am. J. Hum. Genet.* **62:**573-584.

Stoilov I, Akarsu AN and Sarfarazi M (1997) Identification of three different truncating mutations in cytochrome P4501B1 (CYP1B1) as the principal cause of primary congenital glaucoma (buphthalmos) in families linked to the GLC3A locus on chromosome 2p21. *Hum. Mol. Genet.* **6:**641-647.

Stoilov I, Jansson I, Sarfarazi M and Schenkman JB (2001) Roles of cytochrome P450 in development. *Drug Metabol. Drug Interact.* **18:**33-55.

Stoilov I, Rezaie T, Jansson I, Schenkman JB and Sarfarazi M (2004) Expression of cytochrome P4501b1 (Cyp1b1) during early murine development. *Mol. Vis.* **10:**629-636.

Zhang QY, Dunbar D and Kaminsky L (2000) Human cytochrome P-450 metabolism of retinals to retinoic acids. *Drug Metab. Dispos.* **28:**292-297.

Footnotes

Supported in part by NIH grants R01 EY11095, HL67569 and HL70694.

DMD Fast Forward. Published on February 26, 2007 as DOI: 10.1124/dmd.106.014282
This article has not been copyedited and formatted. The final version may differ from this version.

Figure Legends

Figure 1 A, left. Western blot for Cyp1b1 detection in tissues. Track 1, 50 µg adult mouse eye microsomes; track 2, 20 µg spontaneous mouse breast tumor 600 x g supernatant; track 3, 25 µg mouse liver microsomes; track 4, 25 µg P0 whole mouse microsomes; track 5, 0.05 pmol Cyp1b1 protein standard. **A, right.** Western blot titration of Cyp1b1 standards: 200, 100, 50, 25, 10, and 5 fmol (tracks 1-6). **B.** Identification of Cyp1b1 in adult mouse eye microsomes and P0 whole mouse microsomes. Microsomes were subjected to SDS-PAGE as described in Methods and the band corresponding to anti-Cyp1b1 reactive protein was excised, trypsinized, and subjected to LC/MS/MS. Uppermost figure shows peptide fragments of purified Cyp1b1. Middle figure shows an ion fragment of the trypsinized, band corresponding to the antibody-reactive band in whole P0 mouse microsomes. The lower panel shows the blast search results with the sequences of all of the ion fragments identified as from Cyp1b1 (bold).

Figure 2. Visualization of iridocorneal angle (IC) of 6 month old mouse eye with adjacent structures. Slide was of 6 month old C57BL/6 mouse eye photographed at 400X magnification. The slide was reacted with antiserum diluted 1:500 and stained for 10 min, in order to demonstrate lack of CYP1B1 (purple stain) in trabecular meshwork (TM) structure. IN, inner nuclear layer; ON, outer nuclear cell layer; G, ganglion cell layer; ICE, inner ciliary epithelium; I, iris; C, corneal epithelium; TM, trabecular meshwork.

Figure 3. Immunolocalization of Cyp1b1 in mouse eye structures. a-c, 6 month old (P6mo) C57BL/6 mice; d-f, 6 month old albino Swiss Webster mice; g-i, P28 C57BL/6 mice; j-l, P14

C57BL/6 mice. Immunohistochemistry as described in Methods. Slides were photographed at 400X magnification and bars represent 50 μm. C, cornea; ICE, inner ciliary epithelium; G, retinal ganglion cells; IN, retinal inner nuclear layer; OCE, outer ciliary epithelium. Arrows point to immunostaining.

Figure 4. Immunolocalization of Cyp1b1 in P07, P01, E17.5 and E15.5. C57BL/6 mouse eyes. a-c, P07 mice; d-f, P01 mice; g-i, E17.5, and j-l, E15.5 mice. Immunohistochemistry is as described in Methods. Slides were photographed at 400X magnification and bars represent 50 μm. CS, conjunctival space; C, cornea; ICE, inner ciliary epithelium; G, retinal ganglion cells; IN, retinal inner nuclear layer; ON, retinal outer nuclear layer; L, lens; PR, pigmented retinal layer, NR, neural retina, anterior tip of optic cup; EL, eyelid; EC, lens epithelial cells; EN, corneal endothelial cells. Arrows point to immunostaining.

Figure 5. Comparison of Cyp1b1 immunohistochemical stain density in the mouse eye structures during development. Data from Figures 4 and 5 are displayed. See description under Methods.

DMD Fast Forward. Published on February 26, 2007 as DOI: 10.1124/dmd.106.014282
This article has not been copyedited and formatted. The final version may differ from this version.

A

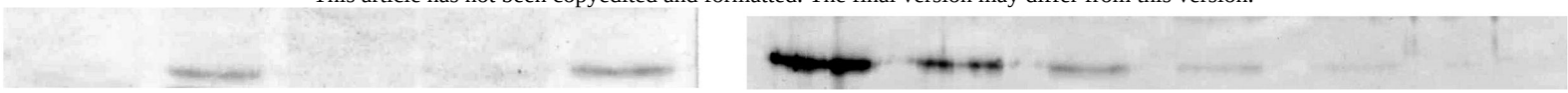

B

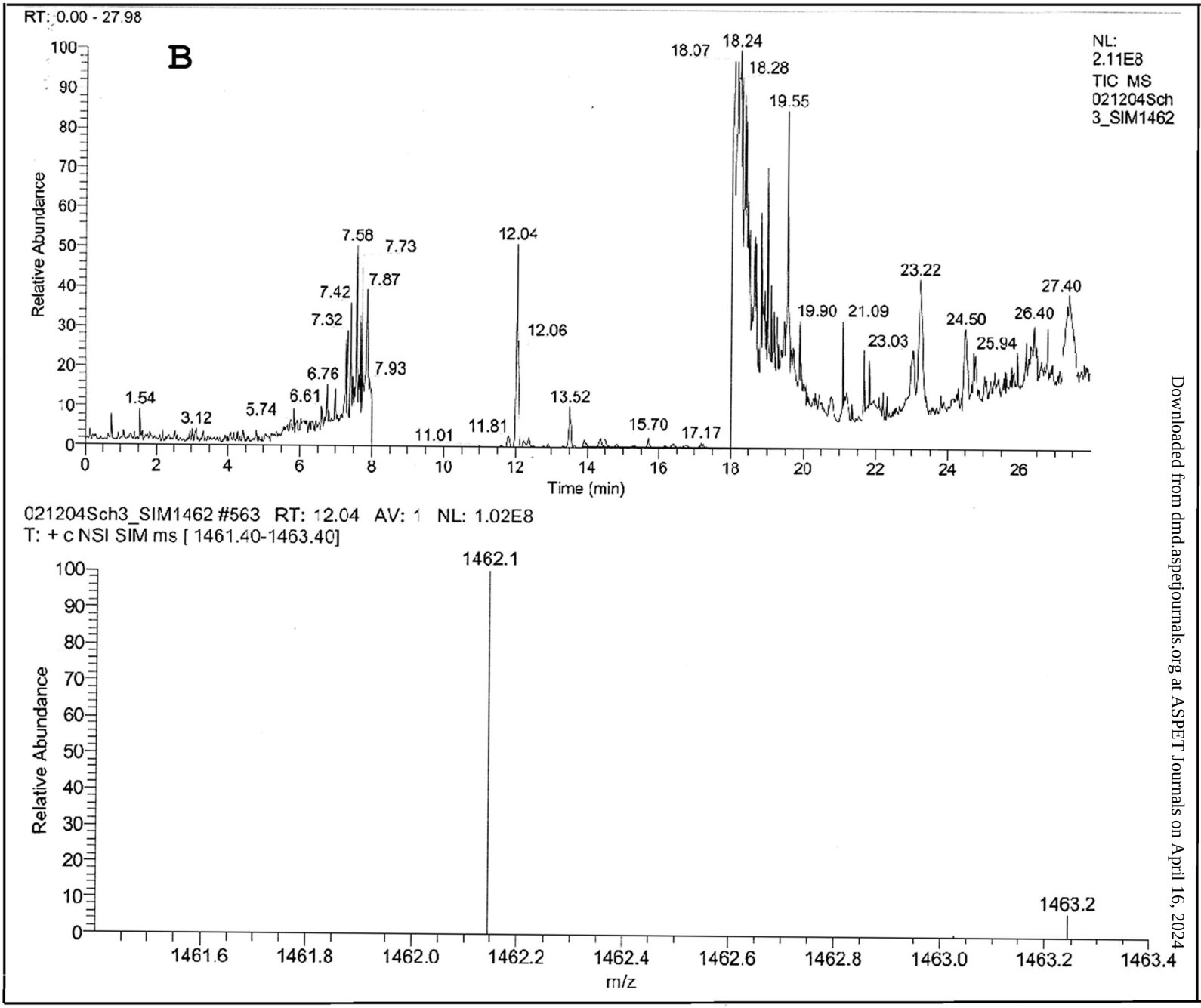

>SW:CP1B_MOUSE Q64429 mus musculus (mouse). cytochrome p450 1b1 (ec 1.14.14.1 (cypib1) (p450cmef) (p450ef). 2/2003 [MASS=60581]

MATSLSADSP QQLSSLSTQQ TTLLLLFSVL AAVHLGQWLL RQWQRKPWSS PPGPFPWPLI GNAAAVGQAS
HLYFARLARR **YGDVFQIRLG** SCPVVVLNGE SAIHQALVQQ GSIFADRPPF ASFRVVSGGR **SLAFGHYSEH**
WKTQRRSAYS TMRAFSTRHP RSR**GLLEGHA LAEARELVAV LVR**RCAGGAF LDPTQPVIVA VANVMSAVCF
GCR**YNHDDAE FLELLSHNEE FGR**TVGAGSL VDVLPWLQLF PNPVRTTFRK **FEQLNRN**FSN FVLDKFLR**HR**
ESLVPGAAPR DMTDAFILSA EKKASGDPGD DSSGLDLEDV PATITDIFGA SQDTLSTALL WLLILFTRY**P**
DVQARVQAEL DQVVGRDRLP CMSDQPNLPY VMAFLYESMR FSSFLPVTIP HATTANTFVL GYYIPKNTVV
FVNQWSVNHD PAK**WPNPEDF DPARFLDKDG FINKALASSV MIFSVGKR**RC IGEELSKMLL FLFISILAHQ
CNFKANQNES SNMSFSYGLT IKPKSFR**IHV SLRESMELLD NAVK**KLQTEE GCK

>average mass = **60581**, pI = **8.54**

Tissue	Position	MH+	Sequence (link: NCBI Blast)
P0 microsmes	131-142	1462.60	SLAFGHYSEHWK
Eye microsomes	455-468	1465.77	ALASSVMIFSVGKR

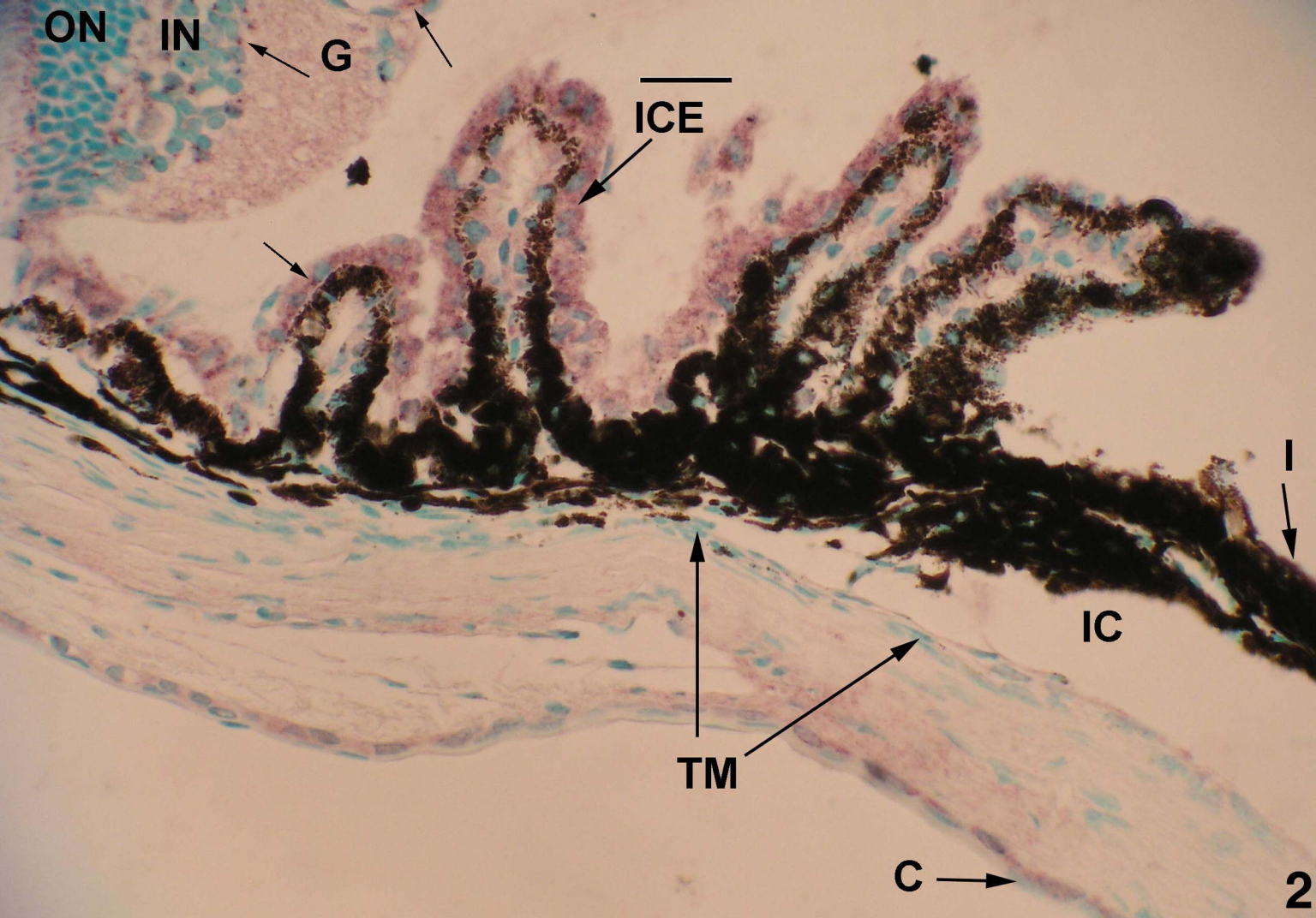
ON
IN
G
ICE
I
IC
TM
C
2

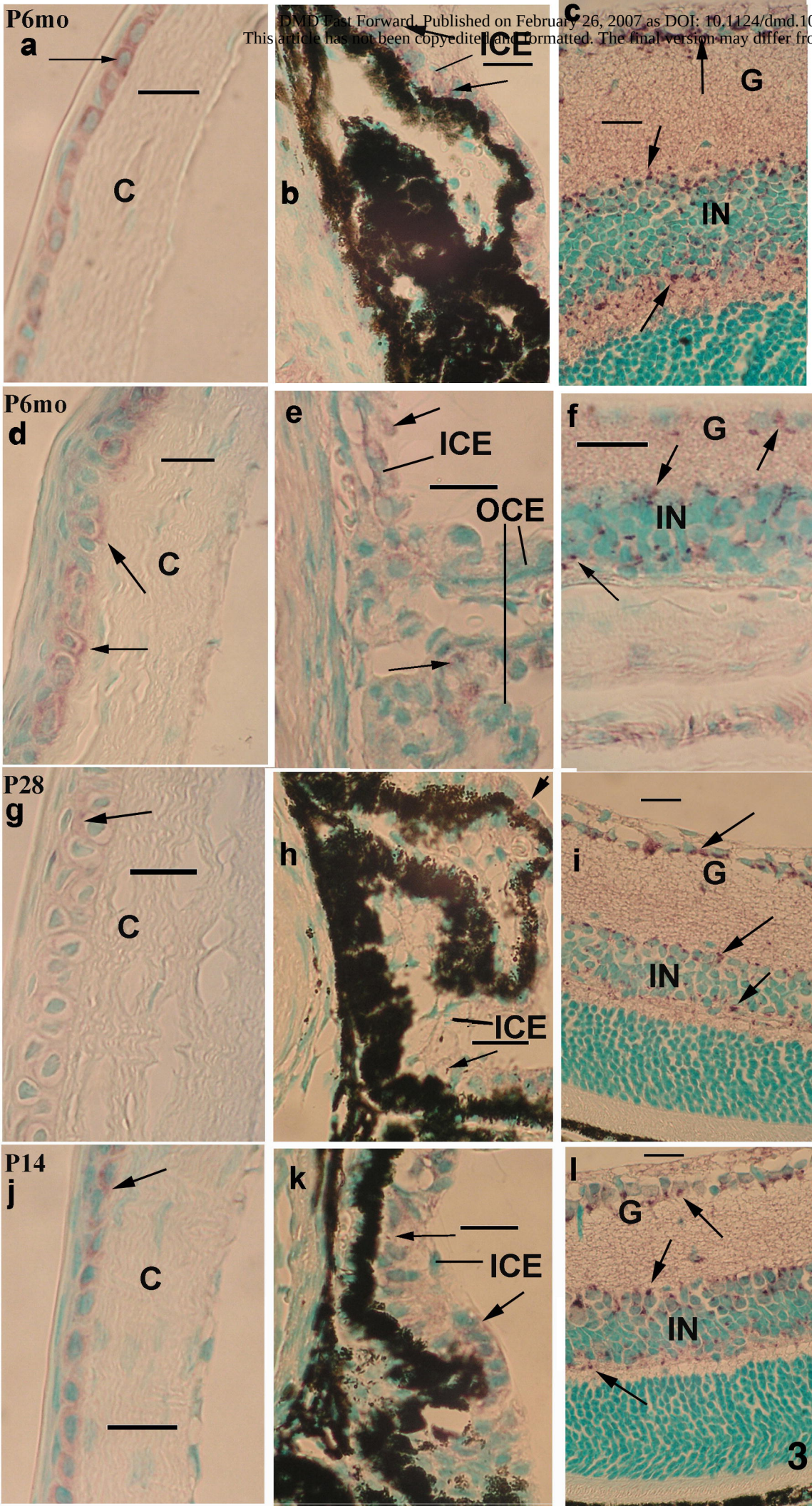

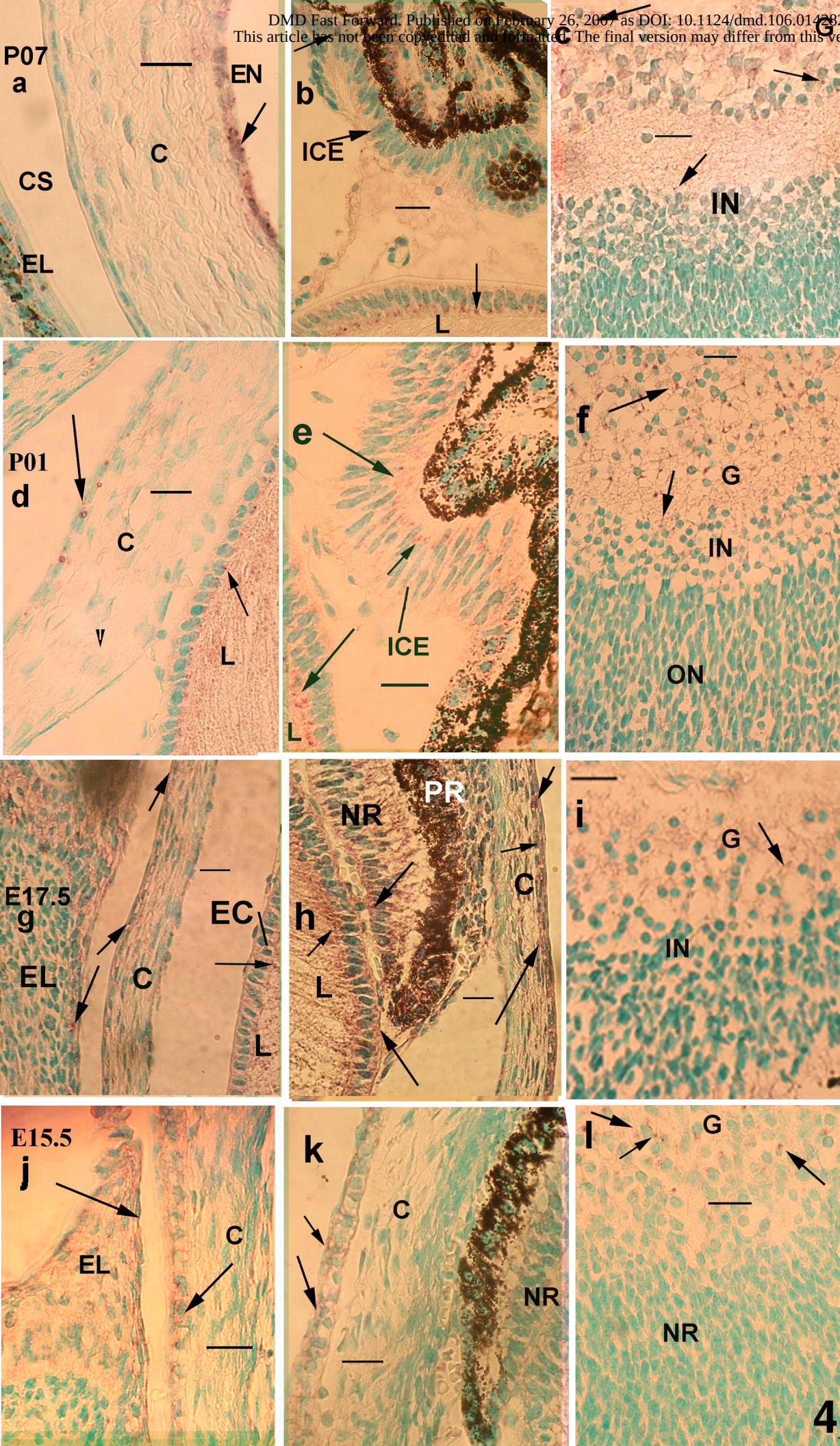

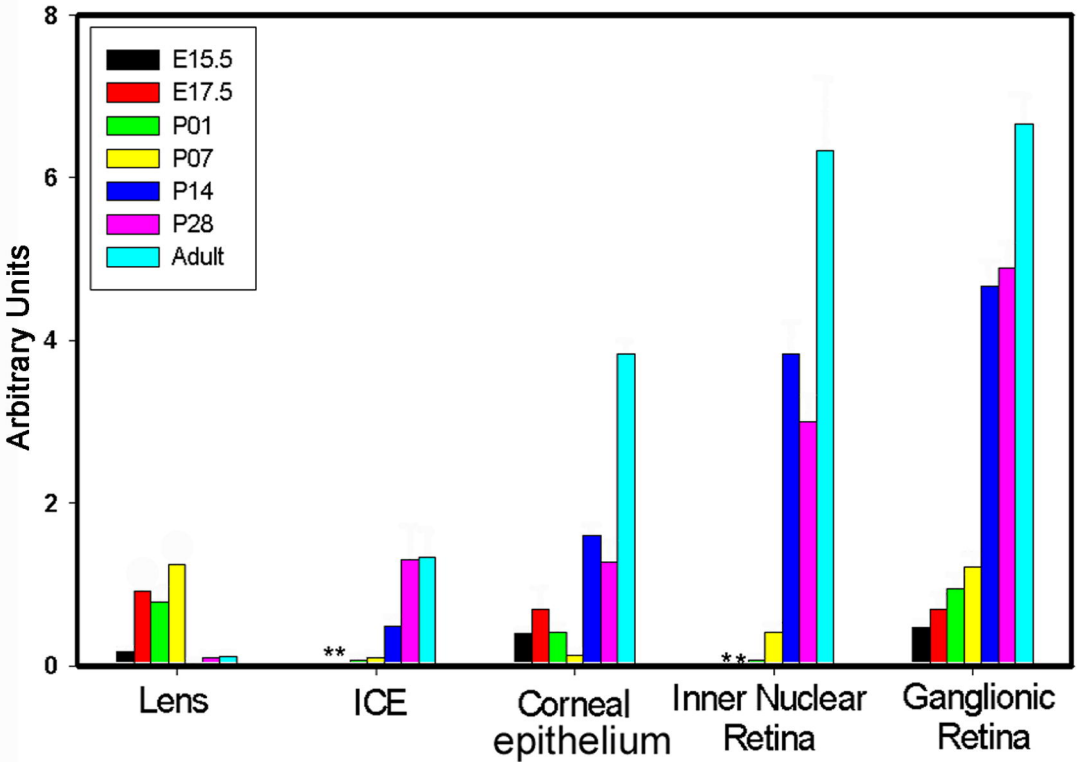
E15.5
E17.5
P01
P07
P14
P28
Adult
Arbitrary Units
8
6
4
2
0
**
**
Lens
ICE
Corneal epithelium
Inner Nuclear Retina
Ganglionic Retina

5